Research Square

Preprints are preliminary reports that have not undergone peer review.
They should not be considered conclusive, used to inform clinical practice,
or referenced by the media as validated information.

A novel parallel approach for solving some free boundary value problems

Amboru Yalamanda
VIT-AP University
Peeyush Singh
peeyushs8@gmail.com

VIT-AP University

Research Article

Keywords:

Posted Date: October 23rd, 2026

DOI: https://doi.org/10.21203/rs.3.rs-11176987/v1

License: This work is licensed under a Creative Commons Attribution 4.0 International License.
Read Full License

Additional Declarations: No competing interests reported.

A novel parallel approach for solving some free boundary value problems

Amboru Yalamanda[1] and Peeyush Singh[2,*]

[1]Department of Mathematics and Statistics,VIT-AP University,AP, India.

[1]E-mails: amboru.24phd7073@vitap.ac.in,susindra.amboru@gmail.com

[2] Department of Mathematics and Statistics,VIT-AP University,AP, India.

[2]E-mails: peeyush.singh@vitap.ac.in,peeyushs8@gmail.com

[*]Corresponding author E-mails: peeyushs8@gmail.com,peeyush.singh@vitap.ac.in

Abstract

This paper introduces a novel, unfied efficient class of parallel direct and indirect iterative framework to solve general obstacle and free boundary value problems. The uniqueness of the solution for the direct parallel method is established under the assumption that the model problem yields an M-matrix. The convergence analysis of the indirect approach is predicated on minimizing the discrete energy functional at each iterative stage of the linear approximation process. Under the aforementioned setting, we establish theoretical convergence results for both smooth and nonsmooth energy functionals defined over a convex set. For the numerical computation of the one-dimensional obstacle problem, we adopt a direct generalized parallel approach based on the SPIKE algorithm.To accelerate convergence and reduce computational complexity, a fast recursive version of the scheme is generalized to the nonsmooth case. For two- and three-dimensional obstacle problems, we employ a directional splitting method that treats each directional subproblem as a one-dimensional obstacle minimization problem. By framing the energy functional minimization as a parabolic time-dependent problem and utilizing an Armijo time-stepping rule during the solution update process, we successfully obtain results for higher-dimensional obstacles. Additionally, this study explores the possibility of extending the algorithm into a constrained quadratic programming optimization solver. We also evaluate the framework on image deblurring phenomena under the aforementioned setting, successfully recovering the original images. Finally, numerical illustrations are provided to validate the theoretical results.

MSC2020 Subject Classification: 65K15, 90C33, 65Y05, 49J40
ACM CCS Concepts: Parallel algorithms; ;Obstacle Problem;Variational Inequality; Free Boundary Value Problem(FBP); Mathematics of Computing Mathematical Software

1 Introduction

In a free boundary problem (FBP), both the partial differential equation and its unknown domain boundary must be solved simultaneously. Such problems frequently arise in physics and engineering, particularly in modeling phase transition phenomena like the melting of ice into water or in tribology problem (see for example [27]) like generation of caviation phenomenon in two moving contacts. The "free" boundary represents the moving interface between distinct phases or regions, such as the liquid-solid interface (or liquid-gas

interface). Another application of free boundary problems arises in financial mathematics specifically in American-style option pricing, where the option value is modeled using an evolutionary variational inequality as well as in game theory as a Nash equilibrium. The brief review and current development in the field is as follows. A rigorous theoretical framework of the obstacle problem originated with Stampacchia and coworkers [2].The regularity result for the model was first proved by Caffarelli [3], who provided a deep analytical understanding of the model. Subsequent numerical developments included finite element discretizations and error estimates [36], augmented Lagrangian and penalty approaches [5], and variational discretization techniques. Subsequently, Scholz [35] implemented this scheme within a penalty finite element approximation framework to derive sharp a priori error bounds. Conforming finite element methods (FEM) are standard for obstacle problems. While linear ($\mathcal{P}_1$) elements offer reliability, accuracy near free boundaries improves with quadratic ($\mathcal{P}_2$) variants in 2D and 3D. A posteriori error estimation and adaptive refinement advanced via localized estimators [6], pointwise error control and barrier sets [7], and optimal convergence proofs for adaptive FEM [8]. Parallel developments in Discontinuous Galerkin (DG-FEM) methods yielded optimal a priori and a posteriori bounds [9, 11, 12], alongside bubble-enriched $\mathcal{P}_2$ implementations in 3D [13]. Parallel to these developments, several independent frameworks leveraging optimization theory have been proposed for solving obstacle problems. For instance, Friedlander and Tseng [14] introduced the exact regularization of convex programs, while Goldstein and Osher [15] developed the split Bregman method for L^1-regularized problems. Iterative solvers became essential for practical computation. Hintermüller, Ito, and Kunisch [17] introduced the primal-dual active set method, demonstrating its equivalence to a specific semismooth Newton-type algorithm. Wang [18] provided finite element error bounds for quadratic elements under strong regularity assumptions, whereas Wang et al. [38] proposed a two-level finite element algorithm that refines solutions near the free boundaries to achieve nearly optimal error bounds. Various domain decomposition methods were explored in the literature for solving the obstacle problem on parallel computers [29]. Basic principal of these decomposition based on partitioning of global spatial domain into subdomains assigned to separate processors via MPI. Projected successive relaxation(PSOR) is well known iterative method for solving the obsatcle problem. Extending these idea on parallel computer many people used PSOR via Red-Black ordering. These ordering breaks data dependencies enabling concurrent cell updates within decoupled subsets. Badaya used Schwarz domain decomposition methods and solve localized obstacle problems, while primal-dual active set (PDAS) strategies reduce inactive regions to standard linear systems for faster solving. Additionally, he proved a convergence of a domain decomposition algorithm and provide convergence rate which based on minimizing quadratic functionals in Hilbert spaces. Various one and two level domain decompostion methods have been studied last couple of decades((for more review in this work see [21, 22]). In 2003 Badaya and coworkers [20] gave first explicit convergence rate estimates for one and two level Schwarz method for variational inequalities. Apart from these developments, some authors employed multi-grid methods for solving the model in the form of the full approximate scheme (FAS) or projected algebraic multigrid (PAMG) [23] to achieve optimal $\mathcal{O}(N)$ algorithmic complexity. In this process spatial domain decomposition scales operations across grid levels, but encounters communication bottlenecks at very coarse hierarchies. Few authors [24, 25] introduced splitting augmented Lagrangian methods for structured monotone variational inequalities with operators composed of two or three separable parts. The primary benefit of this method is that followers can execute their individual subproblems concurrently. Recently, several authors [16] have utilized operator splitting via the alternating direction method of multipliers (ADMM) to reformulate the elliptic state as a pseudo-transient parabolic problem. They applied the splitting frameworks (like ADMM) decouple complex spatial dimensions into independent, explicit directional sweeps, eliminating global linear system updates and matching GPU multithreading models perfectly. A few authors have also endeavored to obtain a discretized solution for the continuous variational inequality that minimizes energy over an admissible set , as well as for its discretized algebraic complementarity system.This is realized by distributing parts of the stiffness matrix across concurrent parallel processing units.

The current work is higly motivated from the work of A. Sameh and coworkers [26, 1] on the develpment of efficient banded solvers SPIKE algorithm. The present study is adopted here due to its exceptional ability to solve large-scale banded linear systems in parallel while balancing communication overhead and computational complexicity cost. The SPIKE algorithm serves as a powerful high-performance computing (HPC) alternative to traditional sequential factorization such as LU decomposition which struggle with scalability issue on modern multiprocessor systems due to their sequential dependencies. These major communication bottlenecks can be easily handle through divide and conquer domain decomposition strategy. The solver offers superior high-performance computing scalability, minimal communication costs, massive speedup, and exceptional algorithmic flexibility. However, its application to constraint optimization has not yet been explored much in details or limited in literature review. The general obstacle problem is a classical problem in the mathematical theory of partial differential equations (PDEs) and variational inequalities. It models physical situations, such as an elastic membrane clamped at the boundary and pushed from below by a rigid obstacle. This article is dedicated to exploring and developing the application of SPIKE dense banded solvers as well as its convergence analysis to constraint optimization problems (obstacle type problems). These applications have not been extensively investigated for constraint minimization problems (or if it has done only treating the problem as linear system sense), which opens an active research direction to reexamine the method and analyze its development as a commercial optimization software tool.

1.1 The classical obstacle model

Let Ω be a bounded domain in $\mathbb{R}^n$ ($n \in \{1, 2, 3\}$) with a smooth boundary $\partial\Omega$. Given the pde model parameters consisting of an obstacle $\psi_{ob} \in L^2(\Omega)$, a boundary profile $g \in H^{1/2}(\partial\Omega)$, and a forcing term $f \in L^2(\Omega)$, we define the set of admissible functions in the form of

$$\mathcal{K} = \{v \in H^1(\Omega) : v|_{\partial\Omega} = g \text{ and } v \geq \psi_{ob} \text{ a.e. in } \Omega\}. \tag{1}$$

To solve the obstacle problem, we minimize an energy functional over the admissible set. We seek a solution $u \in K$ that satisfies

$$\min_{v \in \mathcal{K}} \mathcal{J}(v) := \int_\Omega \left(\frac{1}{2}|\nabla v|^2 - fv\right) dx \tag{2}$$

Alternatively, this is equivalent to the **variational inequality** formulation: find a solution $u \in \mathcal{K}$ such that for all $v \in \mathcal{K}$:

$$\int_\Omega \nabla u \cdot \nabla(v - u)dx \geq \int_\Omega f(v - u)dx \tag{3}$$

Once we enforce regularizition conditions across both domain then it allows the obstacle problem to be stated in its pointwise complementarity form (KKT conditions). A solution u naturally partitions the domain Ω into a contact zone (or coincidence set) $\Omega_C = \{x \in \Omega : u(x) = \psi_{ob}(x)\}$ and a non-contact zone $\Omega_N = \{x \in \Omega : u(x) > \psi_{ob}(x)\}$.
The complementarity form states that solution u must satisfy the following conditions almost everywhere in Ω

$$u \geq \psi_{ob} \tag{4}$$

$$-\Delta u - f \geq 0 \tag{5}$$

$$(u - \psi_{ob}).(-\Delta u - f) = 0 \tag{6}$$

$$u = g \quad \text{on } \partial\Omega \tag{7}$$

To solve the obstacle problem numerically, we discretize the domain Ω using a mesh or grid (e.g., using Finite Difference or Finite Element methods). Let N be the number of interior grid points. The discrete equivalent

to minimizing the energy functional turns out a constrained quadratic programming (QP) problem

$$\min_{\mathbf{u}\in\mathbb{R}^N}\left(\frac{1}{2}\mathbf{u}^T A\mathbf{u}-\mathbf{f}^T\mathbf{u}\right) \quad \text{subject to constrained } \mathbf{u}\geq \boldsymbol{\psi_{ob}}, \tag{8}$$

where $\mathbf{u}, \boldsymbol{\psi} \in \mathbb{R}^N$ are unknown solution and known obstacle respectively. Using the discrete Karush-Kuhn-Tucker (KKT) optimization conditions, the matrix problem reformulated to the continuous complementary form. We seek a solution $\mathbf{u} \in \mathbb{R}^N$ such that

$$\mathbf{u}-\boldsymbol{\psi_{ob}}\geq \mathbf{0} \tag{9}$$

$$A\mathbf{u}-\mathbf{f}\geq \mathbf{0} \tag{10}$$

$$(\mathbf{u}-\boldsymbol{\psi_{ob}}).(A\mathbf{u}-\mathbf{f})=0 \tag{11}$$

In this curreent work, we consider a parallel algorithm approach for a class of obstacle/free boundary value problems. The reminder paper is orgnized as follow: Section 2 present a mathematical background and an overview of the parallel algorithm setup. Section 3 discuss some equivalent formulation, its mathematical justification using M-matrix assumptions and novel formulation of projected parallel algorithms(direct and indirect approach) of the model. Section 4 contains generalized discussion on convergence analysis of parallel algorithms. Section 5 elaborate numerical findings and applications of the algorithm. The final section (Section 6) wraps up the study, restates the main findings, and may suggest limitations and directions for future work.

2 Mathematical distributive description

Let $\mathcal{V}$ be a Banach space that is reflexive and let $\mathcal{J}$ be a convex functional defined as $\mathcal{J}:\mathcal{V}\to\mathbb{R}$. We examine the optimization problem of the form

$$\min_{v\in\mathcal{K}}\mathcal{J}(v):=\int_\Omega\left(\frac{1}{2}|\nabla v|^2-fv\right)dx, \quad \mathcal{K}\subset\mathcal{V}, \tag{12}$$

where $\mathcal{K}$ denotes a closed convex subset of $\mathcal{V}$. In this section, we focuses on the case in which the space $\mathcal{V}$ can be decomposed into a direct sum of subspaces $\mathcal{V}_i$, in other words,

$$\mathcal{V}=\mathcal{V}_1\oplus\mathcal{V}_2\oplus--\oplus\mathcal{V}_r=\sum_{i=1}^{r}\mathcal{V}_i. \tag{13}$$

This means that for any $v\in\mathcal{V}$, there exists a unique $v_i\in\mathcal{V}_i$ such that

$$v=\sum_{i=1}^{r}v_i \tag{14}$$

We solve Eqn (5) by decomposing $\mathcal{K}$ into sum of $\mathcal{K}_i\subset\mathcal{V}_i, i=1,2,..,r$, i.e.,

$$\mathcal{K}=\mathcal{K}_1\oplus\mathcal{K}_2\oplus--\oplus\mathcal{K}_r=\sum_{i=1}^{r}\mathcal{K}_i, \tag{15}$$

where each $\mathcal{K}_i$ can be written as

$$\mathcal{K}_i = \mathcal{K}_{i,in} \oplus \mathcal{K}_{i,mid} \oplus \mathcal{K}_{i,out}. \tag{16}$$

Then the solution of Eqn (5) can be evaluated by solving subparts of the minimization problem as the part of these component sets of each $\mathcal{K}_i$, where $i = 1, 2, .., r.$ in sequentially or parallel. In other words, we can reformulate the minimization problem equivalent two minimization problems namely

$$P_1 : \ \textit{Find } u \in \sum_{i=1}^{r} (\mathcal{K}_{i,in} \oplus \mathcal{K}_{i,out}) \ \textit{such that } \mathcal{J}_1(u) = \min_{v \in \sum_{i=1}^{r} (\mathcal{K}_{i,in} \oplus \mathcal{K}_{i,out})} \mathcal{J}(v) \tag{17}$$

and

$$P_2 : \ \textit{Find } u \in \sum_{i=1}^{r} \mathcal{K}_{i,mid} \ \textit{such that } \mathcal{J}_2(u) = \min_{v \in \sum_{i=1}^{r} \mathcal{K}_{i,mid}} \mathcal{J}(v). \tag{18}$$

3 The projected parallel algorithm

This work focuses on solving equations (9)– (11) on parallel processing systems. Before we solve the parallel problem, we set up the linear complemeatrity problem (LCP) as r blocks of matrices stored across r processors. We then subdivide the complemeatrity system along the main diagonal into r linear sub complementarity problems. Each block has a size of n such that $N = nr$, where r is the total number of available processors. A block substructure $A_i, (i = 1, 2, \ldots, r)$ is constructed here for the original linear complemenatrity system (9)– (11) to create r linear complemeatrity subsystem. The linear complementarity problem Eqn (1) is partitioned into

$$\mathbf{C}_i \mathbf{x}_{i-1} + \mathbf{A}_i \mathbf{x}_i + \mathbf{B}_i \mathbf{x}_{i+1} \geq \mathbf{f}_i, \quad i = 1, 2, \ldots, r \tag{19}$$

$$\mathbf{x}_i \geq \mathbf{0} \tag{20}$$

$$\mathbf{x}_i . (\mathbf{C}_i \mathbf{x}_{i-1} + \mathbf{A}_i \mathbf{x}_i + \mathbf{B}_i \mathbf{x}_{i+1} - \mathbf{f}_i) = 0 \tag{21}$$

,where $\mathbf{A}_i$ is the $n \times n$ block diagonal coefficient matrix of each partition. $\mathbf{x}_i$ and $\mathbf{f}_i$ are $n \times 1$ vectors and $\mathbf{C}_i$,$\mathbf{B}_i$ are accompanied left and right offdiagonal blocks of the size $n \times n$. Note that

$$\mathbf{C}_1 = \mathcal{O}_{n \times n}, \quad \mathbf{B}_r = \mathcal{O}_{n \times n}; \tag{22}$$

$$\mathbf{x}_0 = \mathcal{O}_{n \times 1}, \quad \mathbf{x}_{r+1} = \mathcal{O}_{n \times 1}; \tag{23}$$

$$\mathbf{C}_i = \begin{bmatrix} 0 & \hat{C}_i \\ 0 & 0 \end{bmatrix}_{n \times n}, \quad \mathbf{B}_i = \begin{bmatrix} 0 & 0 \\ \hat{B}_i & 0 \end{bmatrix}_{n \times n}$$

$$\mathbf{x}_i = \left[x_{i,1}, \ldots, x_{i,n} \right]^T, \quad \mathbf{f}_i = \left[f_{i,1}, \ldots, f_{i,n} \right]^T$$

, where B_i is an upper triangular matrix and C_i is a lower triangular matrix. For each partition r, Eqn. (2)

can be reformulated as:

$$\mathbf{A}_i\mathbf{x}_i \geq \mathbf{f}_i - \begin{bmatrix} \mathbf{C}_i\mathbf{x}_{i-1} \\ 0 \\ \vdots \\ 0 \\ \mathbf{B}_i\mathbf{x}_{i+1} \end{bmatrix}_{n\times 1} := \mathbf{f}_{*i}, \quad i = 1, \ldots, r \tag{24}$$

$$\mathbf{x}_i \geq \mathbf{0} \tag{25}$$

$$\mathbf{x}_i.\,(\mathbf{A}_i\mathbf{x}_i - \mathbf{f}_{*i}) = 0 \tag{26}$$

Now, if each matrix $\mathbf{A}_i$ is invertible, then the partitioned linear complementarity systems (LCS) (24)– (26) completely decouple, except for the top and bottom m blocks. This decoupling makes the system well-suited for solving the LCS on concurrent processors independently, inspiring a novel decomposition method for the original matrix $\mathbf{A}$. Our main idea in this article is to provide a novel, equivalent formulation of minimizing functionals based on a monotonic linear transformation of the original problem. In other words, we will provide two equivalent functionals, $J_1(u)$ and $J_2(u)$, which share the same set of minimizers as $J(u)$ (i.e., the same function u minimizes both functionals). To support the convergence analysis of our main algorithm, we introduce essential preliminary results.

Theorem 3.1. *Let A be a $n \times n$ monotone matrix whose off diagonal entries are non positive. If for a given vector x_1 with the property $Ax_1 \geq b$, then $x_1 \geq A^{-1}b$.*

Proof. The proof of this result is a special case of the theorem shown in Varga [10]. □

Theorem 3.2. *Let A be a $n \times n$ nonsingular monotone matrix whose off diagonal entries are non positive. Then solving equation* (9)– (11) *is equivalent solving the complemeatrity system of the form*

$$\begin{cases} SX \geq G \text{ such that } DG = F \\ X \geq 0 \\ (SX - G)X = 0 \end{cases} \tag{27}$$

,where matrix D is a collection of r-partioned A_i diagonal blocks (see Figure 1(a)), in other words

$$D = diag(A_1, .., A_r)$$

and matrix S is a collection of r-partioned I_i identity matrices along the diagonal block

$$\tilde{I} = diag(I_1, .., I_r)$$

corresponding accompanied left and right blocks namely V_i and W_i are computed approximately from system of equation given below (see Figure 1(b))

$$A_i[V_i, W_i] = \begin{bmatrix} 0 & C_i \\ . & 0 \\ . & . \\ . & . \\ 0 & . \\ B_i & 0 \end{bmatrix}. \tag{28}$$

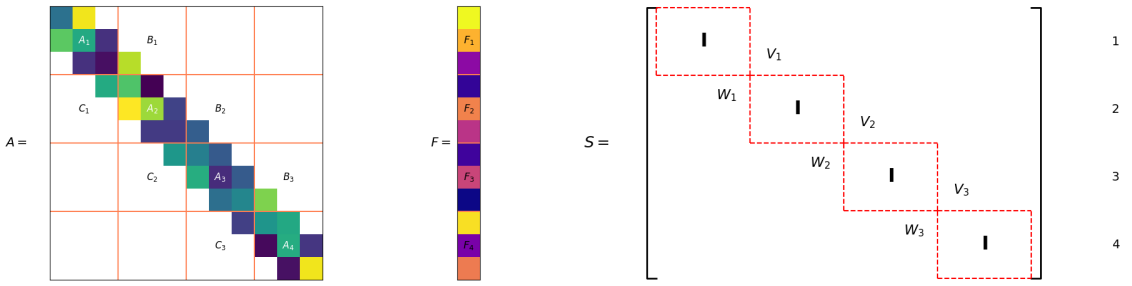


Figure 1: (a)Partitioned matrix $\mathbf{A}$ and right-hand side $\mathbf{F}$ ($r = 4$). (b)S matrix structure with $r = 4$ partition

Proof. The result can be proven easily once it is established that a monotone matrix leaves inequalities invariant under the decomposition described in the theorem. Importantly, such a construction can be implemented because the monotone matrix preserves the inequality by virtue of Theorem 3.1. Hence, without loss of generality, the original problem can be transformed into the form of (32). □

Importantly, the solution of the LCP (31) can be decoupled on a parallel computer and equivalently solved by constructing two sets of minimization problems, namely

- P_1: The first one and its equivalent form are defined as

$$\min_{x \in \sum_{i=1}^{r} \mathcal{K}_{i,in} \oplus \mathcal{K}_{i,out} \subset \mathcal{K}} \mathcal{F}_1 = \frac{1}{2} x^T \tilde{S} x - \tilde{G}^T x$$

$$\Updownarrow$$

$$\begin{cases} \tilde{S}\tilde{X} \geq \tilde{G} \\ \tilde{X} \geq \mathbf{0} \\ (\tilde{S}\tilde{X} - \tilde{G}).\tilde{X} = 0 \end{cases} \tag{29}$$

  where $\tilde{S}, \tilde{G}$ are constructed as from Eqn (32) by considering top β rows and bottom β rows from each partioned block of S, G matrices with total equation size $n_{rd} = 2 * r * \beta$.

- P_2: The second one along with equivalent formulation defined as

$$\min_{x \in \sum_{i=1}^{r} \mathcal{K}_{i,mid} \subset \mathcal{K}} \mathcal{F}_2 = \frac{1}{2} x^T \tilde{I} x - {\tilde{G^*}}^T x$$

$$\Updownarrow$$

$$\begin{cases} \tilde{I}_* X^* \geq G^* \\ X^* \geq \mathbf{0} \\ (\tilde{I}_* X^* - G^*).X^* = 0 \end{cases} \tag{30}$$

The solution to the decoupled minimization problems in Equations (29) and (30) is addressed using both direct and iterative approaches. This section first delineates the algorithm, followed by a formal mathematical justification of its convergence to the exact solution.

3.0.1 Direct projection type iterative parallel approach

We consider the decoupled linear complementarity systems given in (29) and (30), which are analogous to the preprocessing and postprocessing stages of the SPIKE algorithm introduced by Sameh and Polizzi [26, 1]. The reduced linear complementarity system (RLCS) is derived by considering the m top and bottom rows from each r-partitioned block of the SPIKE-type matrix shown in Fig.1(b). The solution of these decoupled problems can be divided into two stages. To solve this reduced LCS, we apply an LU or UL decomposition combined with a projection step in the final stage of the factorization. Once the reduced system is resolved, the remaining solution components associated with Equation (30) can be decoupled straightforwardly. By applying a similar projection in the final stage, we completely recover the full solution vector. To establish the unique solvability of the original LCS problem, we prove the existence of the solution under the assumption that the original matrix A is an M-matrix. Consequently, each partitioned diagonal block is likewise an M-matrix, meaning that the matrix D in the aforementioned decomposition is an M-matrix as well. Therefore, to ensure a unique solution to the original problem, it is sufficient to establish the following theorem, which asserts the desired uniqueness result.

Lemma 3.3. *Let A be a M-matrix and let $A = LU$ and $A = UL$ two decompositions of A. Then $L^{-1} \geq 0, U^{-1} \geq 0$.*

Theorem 3.4. *Let A a be M-matrix then partioned LCS equation* (29) *and* (30) *has a unique solution.*

Proof. Since the original matrix A is an M-matrix, each partitioned diagonal block A_i for all $i = 1, 2, \ldots, r$ is likewise an M-matrix. Consequently, the decoupled block diagonal matrix D remains an M-matrix as it inherits the structural properties of A. Notably, the off-diagonal entries of the SPIKE matrix S are strictly non-positive with moduli strictly bounded by one, which guarantees that S is also an M-matrix. Because S is an M-matrix, extracting its top m and bottom m rows preserves this structure, implying that the reduced matrix $\tilde{S}$ is an M-matrix as well. The existence of the solution to the linear complementarity systems (LCS) (29) and (30) hinges entirely on finding a unique solution to the reduced linear complementarity problem $\mathrm{LCP}(q, \tilde{S})$. Once the reduced solution is computed, the remaining component in (30) yields a unique solution via the trivial identity problem $\mathrm{LCP}(q, \tilde{I}_*)$, which inherently satisfies all M-matrix properties. Therefore, to establish the main result, it is sufficient to prove that the reduced LCS equation (29) possesses a unique solution. By employing a standard LU decomposition combined with a projection onto the convex set, we successfully obtain the unique solution to $\mathrm{LCP}(q, \tilde{S})$. □

Remark 3.5. In essence, the reduced complementarity system preserves a banded structure identical to that of the original problem. Due to its intrinsic recursive nature, this complemeatrity system can be efficiently resolved by executing a recursive routine within the computational algorithm. The procedure of implementation is defined below.

Algorithm 3.6 (**Recursive variants of the algorithm**).

procedure RECURSIVE PROJECTED SPIKE($i_{\text{in}}, i_{\text{out}}, A, x$)

$n_{\text{loc}} \leftarrow i_{\text{out}} - i_{\text{in}} + 1$

if $n_{\text{loc}} \leq \text{tol}$ **then**

Solve LCS

$$(R \cdot y - f_r) \geq 0, \quad y \geq 0, \quad (R \cdot y - f_r) \perp y = 0$$

Return
end if
$m_1 \leftarrow \lfloor n_{\text{loc}}/2 \rfloor; \quad i_{\text{mid}} \leftarrow i_{\text{in}} + m_1 - 1$
RECURSIVE PROJECTED SPIKE$(i_{\text{in}}, i_{\text{mid}}, A, x)$
RECURSIVE PROJECTED SPIKE$(i_{\text{mid}} + 1, i_{\text{out}}, A, x)$
Compute Spike Arrays $V = A^{-1}_{\text{left}} B_1$ and $W = A^{-1}_{\text{right}} B_2$
Solve recollected RLCS

$$(R \cdot y - f_r) \geq 0, \quad y \geq 0, \quad (R \cdot y - f_r) \perp y = 0$$

Compute interface coupling coefficients vector y
$x(i_{\text{in}} : i_{\text{mid}}) \leftarrow \max(x(i_{\text{in}} : i_{\text{mid}}) - V \cdot y_2, 0)$
$x(i_{\text{mid}} + 1 : i_{\text{out}}) \leftarrow \max(x(i_{\text{mid}} + 1 : i_{\text{out}}) - W \cdot y_1, 0)$
end procedure

3.0.2 Iterative Parallel Appraoch

Algorithm 3.7 (**Type I**).

Choose $x^0 \in V$ and $\gamma_1, \gamma_2 > 0$
For $k = 0, 1, ...$ (!Until $\nabla \mathcal{F}_1$ *and* $\nabla \mathcal{F}_2 = 0$).
Decompose the domain as

$$\mathcal{K} = \sum_{i=1}^{r} \mathcal{K}_i$$

Consider a space of decomposition into two parts as

$$\mathcal{K} = \mathcal{K}_1^* \oplus \mathcal{K}_2^*,$$

where $\mathcal{K}_1^* = \sum_{i=1}^{r} \mathcal{K}_{i,in} \oplus \mathcal{K}_{i,out}$ and $\mathcal{K}_2^* = \sum_{i=1}^{r} \mathcal{K}_{i,mid}$.
Compute $y_1^k \in \mathcal{K}_1$ and $y_2^k \in \mathcal{K}_2$ such that

$$\mathcal{F}_1(x^k + \mathcal{P}_{in \oplus out} y_1^k) = \min_{y_1 \in \mathcal{K}_1} \mathcal{F}_1(x^k + \mathcal{P}_{i,in \oplus out} y_1)$$

$$\mathcal{F}_2(x^k + \mathcal{P}_{in \oplus out} y_2^k) = \min_{y_2 \in \mathcal{K}_2} \mathcal{F}_2(x^k + \mathcal{P}_{mid} y_2)$$

$$x^{1,k} = x^k + \mathcal{P}_{in \oplus out} y_1^k$$

$$x^{2,k} = x^k + \mathcal{P}_{mid} y_2^k$$

Determine δ_1^k, δ_2^k from the below update

$$x^{k+1} = x^k + \delta_1^k \mathcal{P}_{in \oplus out} y_1^k + \delta_1^k \mathcal{P}_{mid} y_2^k \tag{31}$$

such that

$$\mathcal{F}(x^{k+1}) \leq \gamma_1 \mathcal{F}_1(x^{1,k}) + \gamma_2 \mathcal{F}_2(x^{2,k}) \tag{32}$$

End

The above last inequality (36) can be ensure by considering suitable parameters δ_1^k, δ_2^k in the either form

- Determine t such that
$$\mathcal{F}(x^{t,k}) = \min(\mathcal{F}_1(x^k), \mathcal{F}_2(x^k))$$

- Using the convexity property of $\mathcal{F}$
$$x^{k+1} = x^k + \delta_1^k \mathcal{P}_{in\oplus out} y_1^k + \delta_1^k \mathcal{P}_{mid} y_2^k = x^k + \gamma_1^k \mathcal{P}_{in\oplus out} y_1^k + \gamma_2^k \mathcal{P}_{mid} y_2^k$$
with $\delta_1 = \gamma_1$ and $\delta_2 = \gamma_2$.

4 General convergence theory for distributive implementation

In this section, we first state and derive the unconstraint optimization formulation defined in Section 1. We will try to establish some convergence for linear type problem.

4.1 Parallel distributive analysis for general elliptic problem : smooth optimization

Additionally, we assume the functionals $\mathcal{F}_1$ and $\mathcal{F}_2$ are K_1-smooth and K_2-smooth, respectively. By the standard Descent Lemma, this property is equivalent to satisfying the following quadratic upper bounds for all $\mathbf{x}, \mathbf{y} \in \mathcal{K}$:

$$\mathcal{F}_1(\mathbf{y}) - \mathcal{F}_1(\mathbf{x}) \leq \langle \nabla \mathcal{F}_1(\mathbf{x}), \mathbf{y} - \mathbf{x} \rangle + \frac{K_1}{2} \|\mathbf{y} - \mathbf{x}\|^2$$

$$\mathcal{F}_2(\mathbf{y}) - \mathcal{F}_2(\mathbf{x}) \leq \langle \nabla \mathcal{F}_2(\mathbf{x}), \mathbf{y} - \mathbf{x} \rangle + \frac{K_2}{2} \|\mathbf{y} - \mathbf{x}\|^2$$

In this section, we assume that the functionals $\mathcal{F}_1$ and $\mathcal{F}_2$ are K_1 and K_2-smooth. By utilizing this standard Lipschitz-continuous gradient property, we invoke the classic descent lemma to establish the convergence of Algorithm 1. We now state and prove the convergence theorem for Algorithm 1.

Theorem 4.1. *Let $\mathcal{F}_1$ and $\mathcal{F}_2$ be functionals that are bounded from below and possess Lipschitz-continuous gradients. Suppose the space $\mathcal{K}$ is decomposed as $\mathcal{K} = \sum_{i=1}^r \mathcal{K}_i$, where each subspace is partitioned into $\mathcal{K}_i = \mathcal{K}_{i,in} \oplus \mathcal{K}_{i,mid} \oplus \mathcal{K}_{i,out}$. Alternatively, let the space be represented as $\mathcal{K} = \mathcal{K}_1^* \oplus \mathcal{K}_2^*$, where $\mathcal{K}_1^* = \sum_{i=1}^r \mathcal{K}_{i,in} \oplus \mathcal{K}_{i,out}$ and $\mathcal{K}_2^* = \sum_{i=1}^r \mathcal{K}_{i,mid}$. Furthermore, let $\mathcal{R}_{in\oplus out} : \mathcal{K} \to \mathcal{K}_1^*$ and $\mathcal{R}_{mid} : \mathcal{K} \to \mathcal{K}_2^*$ be surjective restriction operators, and let $\mathcal{P}_{in\oplus out} : \mathcal{K}_1^* \to \mathcal{K}$ and $\mathcal{P}_{mid} : \mathcal{K}_2^* \to \mathcal{K}$ be linear, injective embedding operators satisfying $\mathcal{P}_{in\oplus out}^T = \mathcal{R}_{in\oplus out}$ and $\mathcal{P}_{mid}^T = \mathcal{R}_{mid}$. Assume that the space decomposition satisfies the following stability condition for some constant $c > 0$:*

$$\|\mathcal{R}_{in\oplus out}\mathbf{x}\|^2 + \|\mathcal{R}_{mid}\mathbf{x}\|^2 \geq c\|\mathbf{x}\|^2 \quad \forall \mathbf{x} \in \mathcal{K}$$

Then, every limit point of the sequence

$$\{\mathbf{x}^k\} := \begin{Bmatrix} \mathbf{x}_1^k \\ \mathbf{x}_2^k \end{Bmatrix}$$

generated by Algorithm 1 is a solution to the minimization problem, satisfying:

$$\lim_{k\to\infty} \nabla\mathcal{F}(\mathbf{x}^k) = \begin{Bmatrix} \lim_{k\to\infty} \nabla\mathcal{F}_1(\mathbf{x}_1^k) \\ \lim_{k\to\infty} \nabla\mathcal{F}_2(\mathbf{x}_2^k) \end{Bmatrix} = \begin{Bmatrix} \mathbf{0} \\ \mathbf{0} \end{Bmatrix}$$

Proof. We observe that

$$\nabla\mathcal{F}_1(y_1) = \nabla\mathcal{F}(x_1^k + \mathcal{P}_{in\oplus out}y_1)\mathcal{P}_{in\oplus out}$$
$$\nabla\mathcal{F}_2(y_2) = \nabla\mathcal{F}(x_2^k + \mathcal{P}_{mid}y_2)\mathcal{P}_{mid}$$

As we assume that $\mathcal{F}_1$ $\mathcal{F}_2$ are Lipschitz continuous gradients with constants K_1 and K_2 we get that

$$||\nabla\mathcal{F}(y_1) - \nabla\mathcal{F}(y_1)|| \leq ||\nabla\mathcal{F}_1(y_1) - \nabla\mathcal{F}_1(y_1)|| + ||\nabla\mathcal{F}_2(y_1) - \nabla\mathcal{F}_2(y_1)||$$

$$= ||\nabla\mathcal{F}(x_1^k+\mathcal{P}_{in\oplus out}y_1)\mathcal{P}_{in\oplus out} - \nabla\mathcal{F}(x_1^k+\mathcal{P}_{in\oplus out}\bar{y}_1)\mathcal{P}_{in\oplus out}|| + ||\nabla\mathcal{F}(x_2^k+\mathcal{P}_{mid}y_1)\mathcal{P}_{mid} - \nabla\mathcal{F}(x_2^k+\mathcal{P}_{mid}\bar{y}_1)\mathcal{P}_{mid}||$$
$$\leq ||\mathcal{P}_{in\oplus out}||.K_1||\mathcal{P}_{in\oplus out}(y_1 - \bar{y}_1)|| + ||\mathcal{P}_{mid}||.K_2||\mathcal{P}_{mid}(y_1 - \bar{y}_1)||$$
$$||\mathcal{P}_{in\oplus out}||^2.K_1||(y_1 - \bar{y}_1)|| + ||\mathcal{P}_{mid}||^2.K_2||(y_1 - \bar{y}_1)||$$
$$\leq K.(||\mathcal{P}_{in\oplus out}||^2 + ||\mathcal{P}_{mid}||^2)||(y_1 - \bar{y}_1)||,$$

here $K = \max(K_1, K_2)$.
which shows that $\nabla\mathcal{F}$ is lipschitz continuous. Let $z_1^k = -(1/K).\nabla\mathcal{F}_1(0)^T$ and $z_2^k = -(1/K).\nabla\mathcal{F}_2(0)^T$. Then by using quardratic Bound lemma we able to get

$$\nabla\mathcal{F}_1(0) - \nabla\mathcal{F}_1(z_1^k) \geq \frac{1}{2K}||\nabla\mathcal{F}_1(0)^T||$$

$$\nabla\mathcal{F}_2(0) - \nabla\mathcal{F}_2(z_2^k) \geq \frac{1}{2K}||\nabla\mathcal{F}_2(0)^T||$$

As we know from the minimization property, $\mathcal{F}_1(z_1^k) \geq \mathcal{F}_1(y_1^k)$ and $\mathcal{F}_2(z_2^k) \geq \mathcal{F}_2(y_2^k)$ implies

$$\mathcal{F}(x^k) - \mathcal{F}(x^{1,k}) \geq \mathcal{F}_1(0) - \mathcal{F}_1(y_1^k) \geq \frac{1}{2K}||\nabla\mathcal{F}_1(0)^T||$$

and

$$\mathcal{F}(x^k) - \mathcal{F}(x^{2,k}) \geq \mathcal{F}_2(0) - \mathcal{F}_2(y_2^k) \geq \frac{1}{2K}||\nabla\mathcal{F}_2(0)^T||$$

which implies that

$$\mathcal{F}(x^k) - \mathcal{F}(x^{1,k}) \geq \frac{1}{2K}||(\nabla\mathcal{F}(x^k)\mathcal{P}_{in\oplus out})^T||^2 = \frac{1}{2K}||\mathcal{R}_{in\oplus out}\nabla\mathcal{F}(x^k)^T||^2$$

and

$$\mathcal{F}(x^k) - \mathcal{F}(x^{2,k}) \geq \frac{1}{2K}||(\nabla\mathcal{F}(x^k)\mathcal{P}_{mid})^T||^2 = \frac{1}{2K}||\mathcal{R}_{mid}\nabla\mathcal{F}(x^k)^T||^2$$

Now we multiply both side by weight factor $\beta_i \in (0, 1)$ and using above argument able to get the following

$$\mathcal{F}(x^k) - (\beta_1\mathcal{F}(x^{1,k}) + \beta_2\mathcal{F}(x^{2,k})) \geq \frac{c\beta}{2K}||\nabla\mathcal{F}(x^k)^T||^2,$$

where $\beta = \min(\beta_1, \beta_2)$.

Now using the linear convergence theory every limit point of $\{x^k\}$ is convergent, that is

$$\lim_{n\to\infty} \nabla\mathcal{F}(x^k) := \begin{Bmatrix} \lim_{n\to\infty} \nabla\mathcal{F}_1(x_1^k) \\ \lim_{n\to\infty} \nabla\mathcal{F}_2(x_2^k) \end{Bmatrix} = \begin{Bmatrix} 0 \\ 0 \end{Bmatrix}.$$

□

Lemma 4.2. *Let $\mathcal{F}_1 : \mathcal{K}_1^* \to \mathbb{R}$ and $\mathcal{F}_2 : \mathcal{K}_2^* \to \mathbb{R}$ are continuously differential functions and let $\{x_1^k\} \subseteq \mathcal{K}_1^*$ and $\{x_2^k\} \subseteq \mathcal{K}_2^*$. If $\mathcal{F}_1$ and $\mathcal{F}_2$ are bound from below and*

$$\mathcal{F}_1(x^k) - \mathcal{F}_1(x^{k+1}) \geq \alpha_1 ||\nabla\mathcal{F}_1(x^k)||^2$$

and

$$\mathcal{F}_2(x^k) - \mathcal{F}_2(x^{k+1}) \geq \alpha_2 ||\nabla\mathcal{F}_2(x^k)||^2$$

Theorem 4.3. *Let the functionals $\mathcal{F}_1$ and $\mathcal{F}_2$ have Lipschitz-continuous gradients, be bounded from below as stated in Lemma 4.2, and be strongly convex with constants C_1 and C_2, respectively. Then, the sequence of iterates $\{\mathbf{x}^k\}$ converges to the unique minimizer $\mathbf{x}^*$ of $\mathcal{F}$ at a linear rate, satisfying*

$$||\mathbf{x^k} - \mathbf{x}^*|| \leq \Big(\frac{2}{C_1}(\mathcal{F}_1(x_1^0) - \mathcal{F}_1(x_1^k))\Big)^{1/2}\Big(1 - \frac{c_1\beta_1 C_1^2}{K^2}\Big)^{k/2} + \Big(\frac{2}{C_2}(\mathcal{F}_2(x_2^0) - \mathcal{F}_2(x_2^k))\Big)^{1/2}\Big(1 - \frac{c_2\beta_2 C_2^2}{K^2}\Big)^{k/2}.$$

Proof. First part of the proof is similar to the result presented by [32]. We now derive the linear root rate of convergence for $\{\mathbf{x}^i\}$. Utilizing the strong convexity of $\mathcal{F}_1$ and $\mathcal{F}_2$, we obtain the following relations

$$||\nabla\mathcal{F}_1(x_1)||||x_1^i - \bar{x}_1|| = ||\nabla\mathcal{F}_1(x_1^i) - \nabla\mathcal{F}_1(\bar{x}_1)||x_1^i - \bar{x}_1|| \geq \nabla\mathcal{F}_1(x_1^i) - \nabla\mathcal{F}_1(\bar{x}_1)(x_1^i - \bar{x}_1) \geq k_1||x_1^i - \bar{x}_1||^2$$

$$||\nabla\mathcal{F}_2(x_2^i)||||x_2^i - \bar{x}_2|| = ||\nabla\mathcal{F}_1(x_2^i) - \nabla\mathcal{F}_2(\bar{x}_2)||x_2^i - \bar{x}_2|| \geq \nabla\mathcal{F}_2(x_2^i) - \nabla\mathcal{F}_2(\bar{x}_1)(x_2^i - \bar{x}_2) \geq k_2||x_2^i - \bar{x}_2||^2$$

This implies

$$\mathcal{F}_1(x_1^i) - \mathcal{F}_1(x_1^{i+1}) \geq \alpha_1 k_1^2 ||x_1^i - \bar{x}_1||^2$$
$$\mathcal{F}_2(x_2^i) - \mathcal{F}_2(x_2^{i+1}) \geq \alpha_2 k_2^2 ||x_2^i - \bar{x}_2||^2$$

Now using quadratic bound lemma we get

$$(\mathcal{F}_1(x_1^i) - \mathcal{F}_1(x_1^{i+1}) \geq \frac{2\alpha_1 k_1^2}{K_1}$$

$$(\mathcal{F}_2(x_2^i) - \mathcal{F}_2(x_2^{i+1}) \geq \frac{2\alpha_2 k_2^2}{K_2}$$

which can be rewrite as

$$\Big(1 - \frac{2\alpha_1 k_1^2}{K_1}\Big)(\mathcal{F}_1(x_1^i) - \mathcal{F}_1(\bar{x}_1)) \geq \mathcal{F}_1(x_1^{i+1}) - \mathcal{F}_1(\bar{x}_1)$$

$$\Big(1 - \frac{2\alpha_2 k_2^2}{K_2}\Big)(\mathcal{F}_2(x_2^i) - \mathcal{F}_2(\bar{x}_2)) \geq \mathcal{F}_2(x_2^{i+1}) - \mathcal{F}_2(\bar{x}_2)$$

Using the same argument iteratively we able to get

$$(\mathcal{F}_1(x_1^i) - \mathcal{F}_1(\bar{x}_1)) \leq \Big(1 - \frac{2\alpha_1 k_1^2}{K_1}\Big)(\mathcal{F}_1(x_1^0) - \mathcal{F}_1(\bar{x}_1))$$

$$(\mathcal{F}_2(x_2^i) - \mathcal{F}_2(\bar{x}_2)) \leq \Big(1 - \frac{2\alpha_2 k_2^2}{K_2}\Big)(\mathcal{F}_2(x_2^0) - \mathcal{F}_2(\bar{x}_2))$$

This implies

$$(\mathcal{F}_1(x_1^i) - \mathcal{F}_1(\bar{x}_1)) + (\mathcal{F}_2(x_2^i) - \mathcal{F}_2(\bar{x}_2)) \leq \Big(1 - \frac{2\alpha_1 k_1^2}{K_1}\Big)(\mathcal{F}_1(x_1^0) - \mathcal{F}_1(\bar{x}_1)) + \Big(1 - \frac{2\alpha_2 k_2^2}{K_2}\Big)(\mathcal{F}_2(x_2^0) - \mathcal{F}_2(\bar{x}_2))$$

Again from strong convexity property we have that

$$(\mathcal{F}_1(x_1^i) - \mathcal{F}_1(\bar{x}_1)) \geq \frac{k_1}{2}||x_1^i - \bar{x}_1||^2 + \nabla\mathcal{F}_1(\bar{x}_1)(x_1^i - \bar{x}_1)$$

$$(\mathcal{F}_2(x_2^i) - \mathcal{F}_2(\bar{x}_2)) \geq \frac{k_2}{2}||x_2^i - \bar{x}_2||^2 + \nabla\mathcal{F}_2(\bar{x}_2)(x_2^i - \bar{x}_2)$$

or

$$||x_1^i - \bar{x}_1|| \leq \Big(\frac{2}{k_1}(\mathcal{F}_1(x_1^i) - \mathcal{F}_1(\bar{x}_1))\Big)^{1/2}$$

$$||x_2^i - \bar{x}_2|| \leq \Big(\frac{2}{k_2}(\mathcal{F}_2(x_2^i) - \mathcal{F}_2(\bar{x}_2))\Big)^{1/2}$$

This implies

$$(\mathcal{F}_1(x_1^i) - \mathcal{F}_1(\bar{x}_1)) + (\mathcal{F}_2(x_2^i) - \mathcal{F}_2(\bar{x}_2)) \leq \Big(1 - \frac{2\alpha_1 k_1^2}{K_1}\Big)(\mathcal{F}_1(x_1^0) - \mathcal{F}_1(\bar{x}_1)) + \Big(1 - \frac{2\alpha_2 k_2^2}{K_2}\Big)(\mathcal{F}_2(x_2^0) - \mathcal{F}_2(\bar{x}_2))$$

Now using above we able to achieve

$$||\mathbf{x^k} - \mathbf{x}^*|| \leq ||x_1^i - \bar{x}_1|| + ||x_2^i - \bar{x}_2|| \leq$$

$$\Big(\frac{2}{C_1}(\mathcal{F}_1(x_1^0) - \mathcal{F}_1(x_1^k))\Big)^{1/2}\Big(1 - \frac{c_1\beta_1 C_1^2}{K^2}\Big)^{k/2} + \Big(\frac{2}{C_2}(\mathcal{F}_2(x_2^0) - \mathcal{F}_2(x_2^k))\Big)^{1/2}\Big(1 - \frac{c_2\beta_2 C_2^2}{K^2}\Big)^{k/2}$$

□

In practice, solving the local minimization problem exactly is often computationally unfeasible. The below theorem give guarantee about the convergence of such solution.

Theorem 4.4. *Let the functionals $\mathcal{F}_1$ and $\mathcal{F}_2$ have Lipschitz-continuous gradients and be bounded from below, as stated in Lemma 4.2. Suppose the space $\mathcal{K}$ is partitioned into two orthogonal subspaces, $\mathcal{K} = \mathcal{K}_1^* \oplus \mathcal{K}_2^*$, as defined in Theorem 4.1. Additionally, assume that the following holds for some constant $c > 0$:*

$$\|\mathcal{R}_{in\oplus out}\mathbf{x}\|^2 + \|\mathcal{R}_{mid}\mathbf{x}\|^2 \geq c\|\mathbf{x}\|^2 \quad \forall\mathbf{x} \in \mathcal{K}$$

Let $\alpha_1, \alpha_2 > 0$, and assume that Algorithm 1 is relaxed to accept an inexact solution $\mathbf{x}^{k+1}$ for the local

minimization problem whenever the following descent conditions hold:

$$\mathcal{F}_1(\mathbf{x}^k) - \mathcal{F}_1(\mathbf{x}^{k+1}) \geq \alpha_1 \|\mathcal{R}_{in\oplus out}\nabla\mathcal{F}_1(\mathbf{x}^k)\|^2$$

$$\mathcal{F}_2(\mathbf{x}^k) - \mathcal{F}_2(\mathbf{x}^{k+1}) \geq \alpha_2 \|\mathcal{R}_{mid}\nabla\mathcal{F}_2(\mathbf{x}^k)\|^2$$

Then, every limit point of the sequence $\{\mathbf{x}^k\}$ *generated by this relaxed algorithm is stationary, that is,*

$$\lim_{k\to\infty} \nabla\mathcal{F}(\mathbf{x}^k) = \begin{Bmatrix} \lim_{k\to\infty} \nabla\mathcal{F}_1(\mathbf{x}_1^k) \\ \lim_{k\to\infty} \nabla\mathcal{F}_2(\mathbf{x}_2^k) \end{Bmatrix} = \mathbf{0}$$

Additionally, if $\mathcal{F}_1$ *and* $\mathcal{F}_2$ *are strongly convex and their gradients are Lipschitz continuous, then* $\lim_{k\to\infty} \mathbf{x}^k = \mathbf{x}^*$*, which is the unique minimizer of* $\mathcal{F}$*.*

Corollary 4.5. *Let* $\mathcal{F}_1$ *and* $\mathcal{F}_2$ *be strongly convex functionals with bounded-below, Lipschitz continuous gradients, satisfying the space decomposition* $\mathcal{K} = \mathcal{K}_1^* \oplus \mathcal{K}_2^*$ *from Theorem 4.1. Furthermore, let the synchronization step in Algorithm 1 be defined by* $\mathbf{x}^{k+1} = \mathbf{x}^k + \gamma_1\mathcal{P}_{\text{in}\oplus\text{out}}y_1^k + \gamma_2\mathcal{P}_{\text{mid}}y_2^k$ *for positive step-sizes* γ_1, γ_2*. Then, the sequence* $\{\mathbf{x}^k\}$ *converges to the unique minimizer* $\mathbf{x}^*$ *of* $\mathcal{F}$ *as* $k \to \infty$ *under either of the following conditions*

$$\gamma = \gamma_1 + \gamma_2 \leq 1 \text{ and } \gamma = \gamma_1 + \gamma_2 < 2$$

, provided the generated spike matrix S *is symmetric.*

Proof. Using the strongly convexity, bounded-below, Lipschitz continuous gradients properties for the functionals $\mathcal{F}_1$ and $\mathcal{F}_2$ we can easily get the above results. □

Next, we apply the above framework to treat the obstacle problem as a nonsmooth optimization problem.

4.2 Parallel distributive analysis for obstacle problem : nonsmooth optimization

Before we describe the convergence analysis of Algorithm 1, we first present the definitions and preliminary lemmas required for our main analysis. we recall the definition of optimality conditions

Definition 4.1 (Optimality Function)**.** Consider our original problem $\min_{x\in\mathcal{K}} \mathcal{F}(x)$ where $\mathcal{F} : \mathcal{V} \to \mathbb{R}$ and $\mathcal{K} \subseteq \mathcal{K}$. A nonconstant, lower semicontinuous mapping $\zeta : \mathcal{K} \to \mathbb{R}$ is termed an optimality function if it satisfies

1. $\zeta(x) \geq 0$ for all $x \in \mathcal{K}$.

2. $\zeta(x) = 0$ whenever $x \in \arg\min_{y\in\mathcal{K}} \mathcal{F}(y)$.

A point $x \in \mathcal{K}$ is classified as stationary with respect to the optimality function ζ if and only if $\zeta(x) = 0$. In the unconstrained, continuously differentiable setting (where $\mathcal{K}_i = \mathcal{V}_i$ and $\mathcal{F}_i \in C^1(\mathcal{V}_i), i = 1, 2$), $\zeta(x)$ simplifies naturally to the standard gradient norm $\|\nabla\mathcal{F}_i(x_i)\|$. Conversely, when constraints dictate that $\mathcal{K}_i, i = 1, 2$ is a closed convex subset of $\mathcal{V}_i, i = 1, 2$, the first-order necessary conditions yield the minimum

principle optimality function

$$\psi(x_i) := -\min_{y_i} \{\langle \nabla \mathcal{F}_i(x_i), y_i - x_i\rangle \mid y_i \in \mathcal{K}_i,\ \|y_i - x_i\|_\infty \le \alpha_i\}. \tag{33}$$

Lemma 4.6. *If x is a stationary point for the optimality function ψ given above equation 33, then x solve the minimization problem of LCS formed in Section 1.*

Lemma 4.7. *[32] Let $\mathcal{F}_1, \mathcal{F}_2$ be strongly convex functionals with lower-bounded, Lipschitz continuous gradients, and let $\mathcal{K}_1^*, \mathcal{K}_2^* \subseteq \mathcal{V}$ be convex subsets. For a given $x_i \in \mathcal{K}_i, i = 1, 2$, let the descent direction $d_i, i = 1, 2$ be defined by*

$$d_i \in \arg\min \{\langle \nabla \mathcal{F}_i(x_i), v_i\rangle \mid v_i \in \mathcal{K}_i - x_i,\ \|v_i\|_\infty \le \alpha_i\}, \forall i = 1, 2. \tag{34}$$

and let $\kappa_i \in \{2^{-m}\}_{m=0}^{\infty}, i = 1, 2$ be the stepsize chosen via the Armijo condition

$$\mathcal{F}_i(x_i) - \mathcal{F}_i(x_i + \kappa_i d_i) \ge -\frac{\kappa_i}{2}\langle \nabla \mathcal{F}_i(x_i), d_i\rangle. \tag{35}$$

Then, the updated point $x_{\text{new},i} = x_i + \kappa_i d_i$ satisfies

$$\mathcal{F}_i(x_i) - \mathcal{F}_i(x_{\text{new},i}) \ge \vartheta(\psi(x_i)), \tag{36}$$

where $\psi(x_i)$ is the minimum principle optimality function defined in (33), and $\vartheta(t_i) = \min\{\frac{1}{2}t_i, \frac{1}{4\alpha_i^2 K_i}t_i^2\}$ serves as a forcing function.

Remark 4.8. The above results are important for accelerating convergence to achieve the optimality condition during iterations. This condition also provides the key concept of treating the problem as a system of time-dependent ODEs, allowing it to be solved using incremental step sizes.

To solve the obstacle problem, we define the distributed optimality function $\zeta : \mathcal{K} \to \mathbb{R}$ by

$$\zeta(x) = \zeta_{\text{in}\oplus\text{out}}(x) + \zeta_{\text{mid}}(x), \tag{37}$$

where $\zeta_{\text{in}\oplus\text{out}} : \mathcal{K}_1^* \to \mathbb{R}_{\ge 0}$ and $\zeta_{\text{mid}} : \mathcal{K}_2^* \to \mathbb{R}_{\ge 0}$ are nonconstant, lower semicontinuous functions satisfying

- $x_1 \in \arg\min_{y \in \mathcal{K}_1^*} \mathcal{F}_1(y) \iff \zeta_{\text{in}\oplus\text{out}}(x_1) = 0.$
- $x_2 \in \arg\min_{y \in \mathcal{K}_2^*} \mathcal{F}_2(y) \iff \zeta_{\text{mid}}(x_2) = 0.$

A point $x \in \mathcal{K}$ is stationary if $\zeta(x) = 0$. Since both components are non-negative, any global minimizer $x^* \in \arg\min_{x \in \mathcal{K}} \mathcal{F}(x)$ necessarily satisfies $\zeta(x^*) = 0$.

Theorem 4.9 (Convergence of the Obstacle Algorithm)**.** *Let $\mathcal{F}_1, \mathcal{F}_2$ be strongly convex functionals with lower-bounded, Lipschitz continuous gradients, and let $\mathcal{K}_1^*, \mathcal{K}_2^* \subseteq \mathcal{V}$ be convex subsets. If the sequence $\{d^i\}$ is bounded, then the sequence $\{x^i\}$ generated by Algorithm 1 either converges to a stationary point x^*, or all of its accumulation points are stationary.*

5 Numerical Experiment

We perform multiple numerical simulations to illustrate the effectiveness of the proposed algorithms. To evaluate their performance, we first conduct tests on obstacle problems utilizing a direct parallel computational approach that incorporates the simple projection methods discussed in Section 3. For the one-dimensional case, employing the direct projected SPIKE algorithm yields the exact solution to the 1D obstacle problem. Initially a naive version of code written (may not be optimized) to solve general linear complementarity problems (LCPs) assuming matrix composed of M-matrix with banded structure. The 1D obstacle problem is solving it exactly by sharing projection information pointwise to each processor. In Table 1 we plot the average time taken for general LCPs with banded structures with varying computational grid or order of matrix size. However, for solving 2D and 3D cases we also have a unified approach utilizing 1D banded structure and solve the problem linewise treating the problem as 1D obstacle. The main advantage going this way helps us to efficiently resolve less regular free boundaries without producing much numerical instabilities coming from free boundaries as generally observed using iterative schemes. The monotonic structure of such parallel decomposition is highly stable and quickly converges to the actual solution. Types of examples are considered here in the present study. We added test cases with smooth and non-smooth obstacle profiles including benchmark examples available from literature review. To solve two- and three-dimensional obstacle problems, we use a directional splitting approach where the 1D SPIKE algorithm acts as a preconditioner, thereby treating each directional subproblem as a sequence of 1D obstacle problems. To solve two- and three-dimensional obstacle problems, we employ a projected gradient descent framework governed by an Armijo backtracking line search approach, which dynamically calculates step parameters based on a sufficient decrease in the energy functional. The converged residual per iteration illustrates that schemes are highly stable during the iterative process. Another way to solve this problem is to make minimizing energy functional semismooth by adding some penalty functional terms and solving the problem as a smooth minimization problem. Handling these penalties needs a lot of care as the penalty may create an ill-conditioning system if it is combined with an update matrix which accumulates near the free boundary with abrupt change. We treat the penalty implicitly while solving these model examples. We then extend these experiments for general obstacle problems in $\mathbb{R}^n, n = 1, 2, 3$ with a parallel iterative algorithm mentioned in Section 3. We also investigate some continuum structural mechanics examples to test the performance of the parallel schemes. Finally, we assess the performance of the algorithms on practical image deblurring problems. All numerical computation done in this paper on the personal laptop of authors with the following configurations **Intel(R) Core(TM) i5-9300H CPU @ 2.40GHz** (**CPU(s):8 NUMA node0 CPU(s):0–7**).

5.1 Numerical example of obstacle problem $\mathbb{R}^n, n = 1, 2, 3$

Example 1. *Let* $(\Omega, f, \phi) = \big((0,1), 0, \infty\big)$*, and introduce the bilinear form* $a(\cdot,\cdot)$ *given by*

$$a(u,v) = \int_0^1 u'(x)v'(x)dx.$$

We consider two alternative obstacle profile $\Psi_{ob}(x)$ *here as piecewise smooth profiles 38(a):*

$$\Psi_{ob}(x) = \begin{cases} 50\sin^2(2\pi x) & \text{for } 0 \le x \le 0.25, \\ 50\cos^2(2\pi(x-0.25)) & \text{for } 0.25 < x \le 0.5, \\ \Psi_{ob}(1-x) & \text{for } 0.5 < x \le 1, \end{cases} \quad \text{and} \quad \Psi_{ob}(x) = \begin{cases} 10(e^{4x}-1) & \text{for } 0 \le x \le 0.25, \\ 10(e-1) + 20(x-0.25)^2 & \text{for } 0.25 < x \le 0.5, \\ \Psi_{ob}(1-x) & \text{for } 0.5 < x \le 1, \end{cases} \tag{38(a)}$$

Table 1: Projected SPIKE result from 2, 4 and 8 processors and for matrix order$n \times n$ where $n = 16, 32, 64, 128, 512, 1024, 2048, 4096, 8192$ bandwidth $\beta = 2$.

Grid size $n \times n$	No of processors	(CPU-time in Sec ave)	(CPU-time in Hours ave)
16	2	$1.2564105000000001 \times 10^{-3}$	$3.4900291666666671 \times 10^{-7}$
16	4	$1.4426392500000000 \times 10^{-3}$	$4.0073312500000002 \times 10^{-7}$
32	2	$1.7317710000000000 \times 10^{-3}$	$4.8104749999999997 \times 10^{-7}$
32	4	$2.1030914999999998 \times 10^{-3}$	$5.8419208333333333 \times 10^{-7}$
32	8	$3.2978951250000003 \times 10^{-3}$	$9.1608197916666672 \times 10^{-7}$
64	2	$6.3709365000000004 \times 10^{-3}$	$1.7697045833333335 \times 10^{-6}$
64	4	$4.4428387500000006 \times 10^{-3}$	$1.2341218750000002 \times 10^{-6}$
64	8	$7.8692155000000003 \times 10^{-3}$	$2.1858931944444447 \times 10^{-6}$
128	2	$1.2333342000000001 \times 10^{-2}$	$3.4259283333333336 \times 10^{-6}$
128	4	$1.3762024749999999 \times 10^{-2}$	$3.8227846527777777 \times 10^{-6}$
128	8	$8.9567842500000005 \times 10^{-3}$	$2.4879956250000003 \times 10^{-6}$
256	2	$4.2950179000000005 \times 10^{-2}$	$1.1930605277777780 \times 10^{-5}$
256	4	$4.2253353250000000 \times 10^{-2}$	$1.1737042569444444 \times 10^{-5}$
256	8	$5.2808312000000003 \times 10^{-2}$	$1.4668975555555557 \times 10^{-5}$
512	2	0.23135659549999998	$6.4265720972222213 \times 10^{-5}$
512	4	0.13779315225000000	$3.8275875625000000 \times 10^{-5}$
512	8	0.23980285312500002	$6.6611903645833335 \times 10^{-5}$
1024	2	0.94131520550000003	$2.6147644597222222 \times 10^{-4}$
1024	4	0.31377938049999998	$8.7160939027777776 \times 10^{-5}$
1024	8	0.26540373987499999	$7.3723261076388886 \times 10^{-5}$
2048	2	7.7126638784999999	$2.1424066329166665 \times 10^{-3}$
2048	4	1.6991023162500001	$4.7197286562500004 \times 10^{-4}$
2048	8	1.1280106016250002	$3.1333627822916675 \times 10^{-4}$
4096	2	147.86486831849999	$4.1073574532916664 \times 10^{-2}$
4096	4	12.171439289000002	$3.3809553580555563 \times 10^{-3}$
4096	8	7.4110701309999989	$2.0586305919444441 \times 10^{-3}$
8192	2	1861.0646910930000	0.51696241419250000
8192	4	171.62190361750001	$4.7672751004861111 \times 10^{-2}$
8192	8	77.764998189499991	$2.1601388385972219 \times 10^{-2}$

Example 2. *Let* $(\Omega, f, \phi_{ob}) = \big((0,1), 0, \infty\big)$*, where the bilinear form* $a(\cdot,\cdot)$ *is given by*

$$a(u,v) = \int_0^1 u'(x)v'(x)dx.$$

We discuss the numerical study using two separate step-function for the obstacle profile

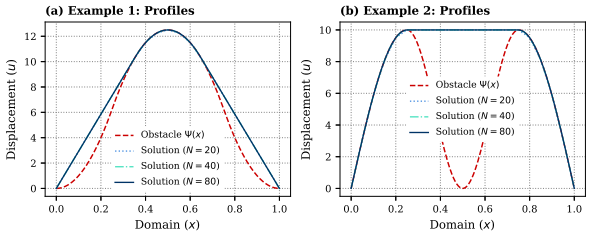
$$\Psi_1(x) = \begin{cases} 1 & \textit{if } 0.35 \le x \le 0.65, \\ 0 & \textit{otherwise.} \end{cases} \quad \textit{and} \quad \Psi_2(x) = \begin{cases} 0.8 & \textit{if } 0.2 \le x \le 0.4, \\ 0.4 & \textit{if } 0.6 \le x \le 0.8, \\ 0 & \textit{otherwise.} \end{cases} \tag{38(b)}$$

To verify the precision of the numerical implementations against an exact baseline, a one-dimensional variant of the obstacle problem is evaluated on $\Omega = (-1, 1)$ with zero boundary conditions under zero external force ($f = 0$). The rigid parabolic lower obstacle is defined as $\psi(x) = 1 - 2x^2$. The exact analytical solution is given by

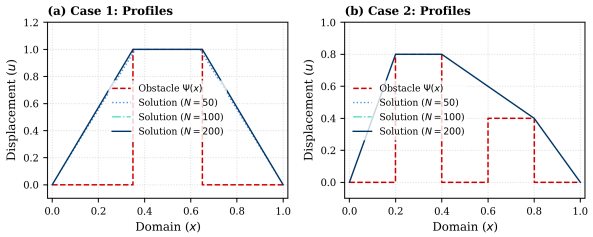
$$u(x) = \begin{cases} 1 - 2x^2 & \text{for } |x| \le x_0, \\ A(1 - |x|) & \text{for } x_0 < |x| \le 1, \end{cases} \tag{39}$$

where the exact transition parameters are $x_0 = 1 - \frac{\sqrt{2}}{2} \approx 0.292893$ and $A = 4 - 2\sqrt{2} \approx 1.171573$. The benchmark solution of obstacle for 1D case is done by direct approach using exactly in one step. However, for higher dimensional check we also did iterative computation too. The below Figure 2d is demonstrated to illustrate the numerically calculated solution profile and the iterative error performance for the semismooth and nonsmooth version error comparison.

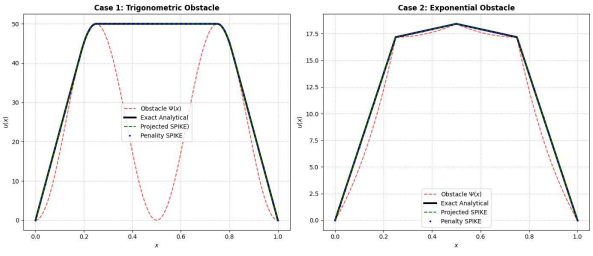
Example 3. *Now we consider an obstacle problem formulated on the square domain* $\Omega = [-2, 2] \times [-2, 2]$*, with the obstacle function* $\Psi(x)$ *defined as in [28].*



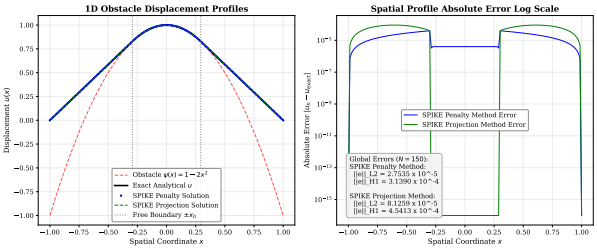
(a) Top left image.



(b) Displacement profiles for the cases 38(b)



(c) Displacement profiles for the cases 38(a)



(d) One-dimensional analytical.

Figure 2: Multi-panal 1D solution profile performance using projected SPIKE (a) Using reference case [35] (b) Example 2 case solution profile (c) Example 1 case solution profiles (d) One-dimensional analytical validation on a uniform grid ($N = 150$). Left Figure: 1D solution profile $u(x)$ and the rigid obstacle. Right figure: Absolute Numerical error $|u_h - u_{\text{exact}}|$.

Example 4. *To examine the convergence and behavior of our method in the presence of non-smooth obstacles, we consider a composite geometric obstacle function defined by in [28]*

A stable solutions are observed and illustrated in the Figure 6 along with their absolute error plot for above Example 3 and Example 4. 3D obsatcle results are also presented in two scenarios demonstrated in Figure

Example 5. *We first consider a smooth, continuous spherical dome obstacle nested at the core of the domain workspace. The geometric constraint profile $\phi_{smooth}(x, y, z)$ is defined analytically by*

$$\phi_{smooth}(x, y, z) = \begin{cases} \sqrt{R^2 - (x^2 + y^2 + z^2)} & \text{if } \sqrt{x^2 + y^2 + z^2} \leq R \\ -1.0 & \text{otherwise} \end{cases} \tag{40}$$

where the radius parameter is locked to $R = 0.8$.

Example 6. *To evaluate the solver under extreme geometric conditions where classical derivative evaluations collapse, we introduce a non-differentiable, sharp four-sided pyramid configuration characterized by a discontinuous subgradient singular peak and sharp crease intersections. The boundary profile $\phi_{nonsmooth}(x, y, z)$ is defined mathematically as:*

$$\phi_{nonsmooth}(x, y, z) = \max\left(-0.4,\ 1.0 - |x| - |y| - |z|\right) \tag{41}$$

To alleviate numerical grid locking across the sharp derivative ridge lines, a regularized smoothing parameterization factor $\epsilon = 10^{-4}$ is introduced into the projection operator loop. This smooths the discontinuous

subgradients into an asymptotic localized boundary layer.

A stable solution profile and error plots of Example 5 and Example 6 are demonstrated in Figure 7. We tried to extend this idea to get solutions of some benchmark 2D and 3D examples are explained below.

Example 7 (volcano-type obstacle)**.** *We consider here a membrane problem over a volcano-type obstacle on the domain* $\Omega = (-1.5, 1.5)^2 \subset \mathbb{R}^2$ *with homogeneous Dirichlet boundary conditions* $u = 0$ *on* $\partial\Omega$ *with obstacle of following form*

$$\psi_{ob}(x,y) = \begin{cases} \max\left(0.22,\, 0.35 - 4.0\left(\sqrt{x^2+y^2} - 0.6\right)^2\right) & \text{for } \sqrt{x^2+y^2} \le 1.1, \\ -0.2 & \text{for } \sqrt{x^2+y^2} > 1.1. \end{cases} \tag{42}$$

A uniform downward gravitational load $f = -\lambda$ *is applied across the domain, leading to the constant and regularized penalization equations defined as*

$$\begin{aligned} \mathbf{A}_{topology}\mathbf{u}_h &\ge \mathbf{f} \\ \mathbf{u}_h &\ge \psi_{\mathbf{ob}} \\ \mathbf{u}_h^T.(\mathbf{A}_{topology}\mathbf{u}_h - \mathbf{f}) &= 0 \end{aligned} \tag{43}$$

and

$$-\Delta u_h + \gamma \min(0, u_h - \psi_{ob}) = -\lambda \quad \text{in } \Omega, \tag{44}$$

where $\gamma = 5 \times 10^6$ *is the penalty parameter, and the system is discretized using standard five-point second-order finite differences on a uniform grid of size* 100×100.

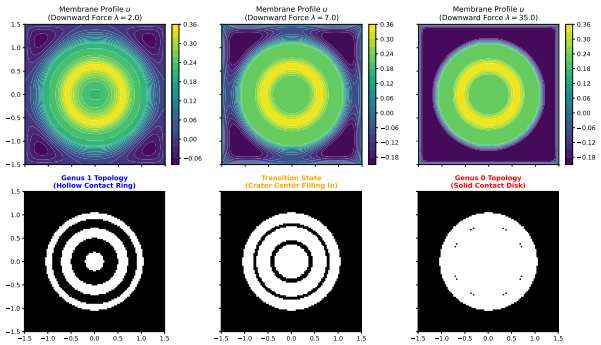


Figure 3: Numerical test of the topological change under increasing downward force λ.**Top row of plots :** continuous solution of membrane displacement profiles u. **Bottom row of plots :** characteristic function of the active contact zone $\Omega_\Lambda = \{x \in \Omega : |u(x) - \psi(x)| < 5 \times 10^{-3}\}$ where variation $\lambda = 2.0, 7.0, 35.0$, the topology smoothly changes from a doubly connected ring (genus 1) to a simply connected solid disk (genus 0).

The numerical results and corresponding active contact sets $\Omega_\Lambda := \{x \in \Omega : u_h(x) = \psi(x)\}$ are illustrated in Fig. 3 across three varying load conditions: The illustrations describe the perfect transition from an annular structure to a solid compact disk without any grid-locking or standard cell-distortion failure modes which generally appear in explicit curve-tracking schemes.

Example 8 (Navier-Cauchy Equations of Linear Elasticity)**.** *We take three-dimensional solid continuum*

Grid Size	Mesh Step (h)	L^2 Error	L^2 Rate (r)	H^1 Error	H^1 Rate (r)
16×16	0.0588	4.7200e-06	—	1.5063e-03	—
32×32	0.0303	1.2650e-06	2.00	8.1614e-04	0.92
64×64	0.0154	3.2690e-07	2.00	4.2646e-04	0.96
128×128	0.0078	8.3053e-08	2.00	2.1822e-04	0.98
256×256	0.0039	2.0929e-08	2.00	1.1041e-04	0.99

Table 2: Numerical error convergence analysis against a reference grid baseline ($N_{ref} = 512$).

mechanics example here to demonstrate the method solution capability for the implicit semi-smooth penalty solver as well as projection solver. we extend the formulation to a three-dimensional solid continuum. This framework is simple adoption of the model problem to a system of coupled vector partial differential equations governed by the classical Navier-Cauchy equations of linear elasticity

$$-\mu \boldsymbol{\Delta} \mathbf{u} - (\lambda_{Lamé} + \mu) \nabla (\nabla \cdot \mathbf{u}) = \mathbf{f} \quad in\ \Omega, \tag{45}$$

where vectors $\mathbf{u} = [u_x, u_y, u_z]^T$ *and* $\mathbf{f} = [0, 0, -\lambda]^T$ *are the structural spatial displacement vector field and a uniform vertical body force represent gravitational load with magnitude* $\lambda = 15.0$*. The material constants* $\lambda_{Lamé}$ *and* μ *represent the Lamé parameters, which are derived from a standard steel/concrete material scale with Young's Modulus* $E = 2.0 \times 10^5$ *and Poisson's ratio* $\nu = 0.3$

$$\lambda_{Lamé} = \frac{E\nu}{(1+\nu)(1-2\nu)}, \quad \mu = \frac{E}{2(1+\nu)}, \tag{46}$$

where Ω *represent computation domain* $\Omega = (-1.5, 1.5)^2 \times (0, 1) \subset \mathbb{R}^3$*. The boundary conditions are distributed to model a block pressed downward onto a rigid foundation, top surface (*$z = 1$ $\mathbf{u} = \mathbf{0}$*, Bottom Surface (*$z = 0$*) Allowed to deform freely along the vertical axis within the interior, subject to a rigid, non-penetration spherical obstacle constraint embedded from below. To guarantee uniqueness and prevent matrix rank singularity, the outer bounding rim of the base is fixed to zero and lateral cladding (*$x = \pm 1.5$*,* $y = \pm 1.5$*) left unconstrained to allow lateral Poisson expansion under vertical pressure. The vertical displacement constraint on the interior of the bottom face (*$z = 0$*) takes the form of a lower bound inequality constraint*

$$u_z(x, y, 0) \geq \psi_{ob}(x, y), \tag{47}$$

where $\psi(x, y)$ *represents the rigid spherical dome surface geometry centered beneath the block coordinates*

$$\psi_{ob}(x, y) = \sqrt{\max\left(0.0,\, R_{sphere}^2 - (x^2 + y^2)\right)} + z_{center}, \tag{48}$$

with a sphere radius $R_{sphere} = 2.0$ *and vertical center shift* $z_{center} = -1.8$*.*

The developed structural mechanics displacement solution profile and the corresponding active contact footmark are demostrated in Fig. 4 using finite difference method with uniform mesh grid $20 \times 20 \times 10$. The constraint and algebraic regularized constraint systems are presented as

$$\begin{aligned} \mathbf{A}_{\text{elastic}} \mathbf{u}_h &\geq \mathbf{f} \\ \mathbf{u}_h &\geq \psi_{\mathbf{ob}} \\ \mathbf{u}_h^T . (\mathbf{A}_{\text{elastic}} \mathbf{u}_h - \mathbf{f}) &= 0 \end{aligned} \tag{49}$$

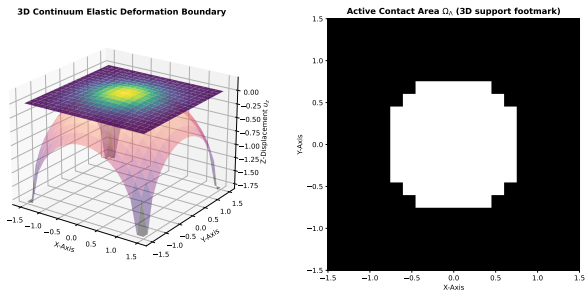


Figure 4: Numerical solution of the three-dimensional continuum linear elasticity obstacle problem for $\lambda = 15.0$. **Left Figure:** Solution profile describing surface u_z movement upward side of the elastic body as it smoothly deforms along the obsatcle ψ_{ob}. **Right Figure:** White color of the discrete active contact domain Ω_Λ that is where $(u_z(x, y, 0) = \psi_{ob}(x, y))$ and black color represent unconstrained free zone that is where strict inequality constraint $u_z(x, y, 0) > \psi_{ob}(x, y)$.

and

$$\mathbf{A}_{\text{elastic}}\mathbf{u}_h + \mathbf{P}(\mathbf{u}_h)\mathbf{u}_h = \mathbf{f} + \mathbf{P}(\mathbf{u}_h)\psi_{\text{ob}}. \tag{50}$$

The 3D surface plot (left figure) emphasizes the smooth vertical deformation field as the elastic block sags under gravity and molds perfectly to the contour of the spherical dome. The active contact footmark $\Omega_\Lambda := \{(x, y) \in \text{int}(\Omega_0) : |u_z(x, y, 0) - \psi_{ob}(x, y)| < 10^{-4}\}$ is mapped in the right figure.

Table 3: Mesh Error in L^2 and H^1 Norm Distributed SPIKE Projection Method in iterative version

Model Problem	**Grid size**	**Total Mesh Points**	L^2 **Norm**	H^1 **Norm**
1D Elastic String	$N_x = 160$	160	6.09126E-03	2.65416E-02
2D Elastic Membrane	$N_x = 60, N_y = 60$	3,600	2.50456E-03	7.05243E-02
3D Elastic Volume	$N_x = 40, Ny = 40, Nz = 40$	64,000	8.03456E-03	9.51456E-02

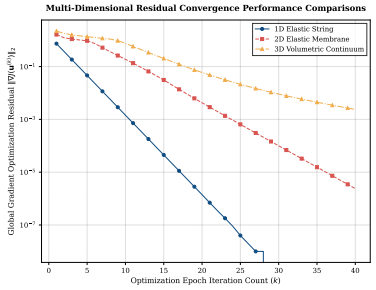
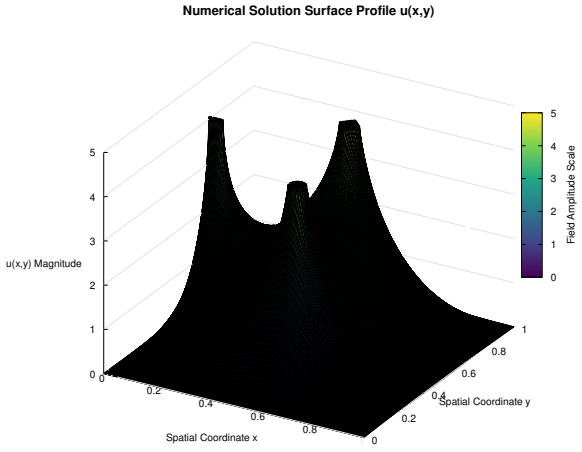


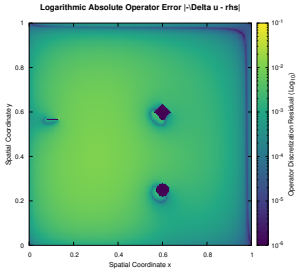
Figure 5: Error residual decay on log scale ($\|R(\mathbf{u}^{(k)})\|_2$) across all spatial dimensional scales.

5.2 Application of parallel algorithm image deblurring problem

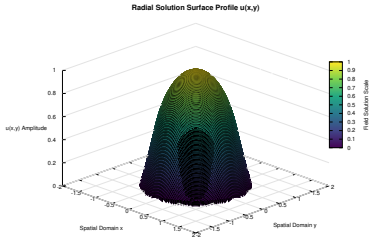
A simple image deblurring model is considered as a practical application here. The model problem is formulated as a bound-constrained linear least-squares problem, where P denotes the blurring matrix, $\mathbf{q}$



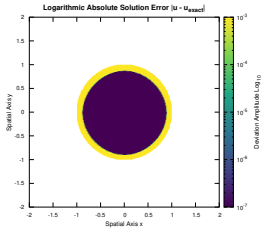
(a) Numerical solution surface $u(x, y)$.



(b) Absolute discretization error $|\Delta u - \text{rhs}|$.

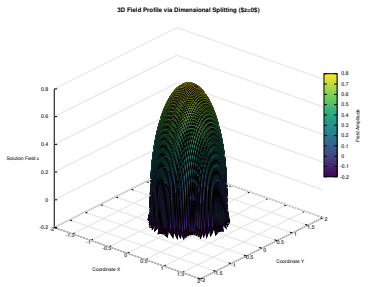


(c) Numerical solution surface $u(x, y)$.

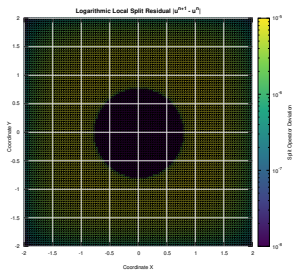


(d) Absolute discretization error $|\Delta u - \text{rhs}|$.

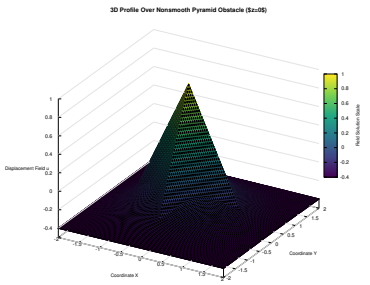
Figure 6: Multi Plot examples of 2D obstacle from available literature review smooth and nonsmooth test cases



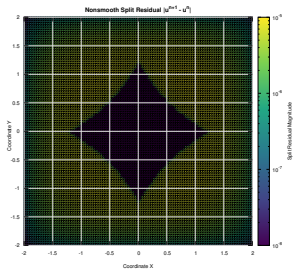
(a) 3D Obstacle Problem a snapshot splitting method



(b) 3D Obstacle Problem error a snapshot splitting method



(c) 3D Obstacle Problem a snapshot splitting method nonsmooth case



(d) 3D Obstacle Problem error a snapshot splitting method nonsmooth case

Figure 7: 3D obstacle and absolute error snapshots for smooth and nonsmooth cases.

represents the observed image containing artifacts, and the solution is subject to the box constraint $\mathbf{0} \leq \mathbf{x} \leq \mathbf{1}$. A two-dimensional image deblurring task governed by a non-diagonal-dominant low-pass Gaussian convolution filter kernel

$$b(\mathbf{x}) = \mathcal{K} * u(\mathbf{x}) + \eta \tag{51}$$

We mapped this operator on distributed memory parallel systems. Using 1D horizontal marching with fixed low-step under-relaxation scaling modifier ($\omega = 0.05$), we produced the deblurred images. The final reconstructed scalar intensity grid (Fig. 8) drives the system residual norm smoothly from 85.29 down to 42.78, preserving continuous spatial phase characteristics across all subdomain rank boundaries.

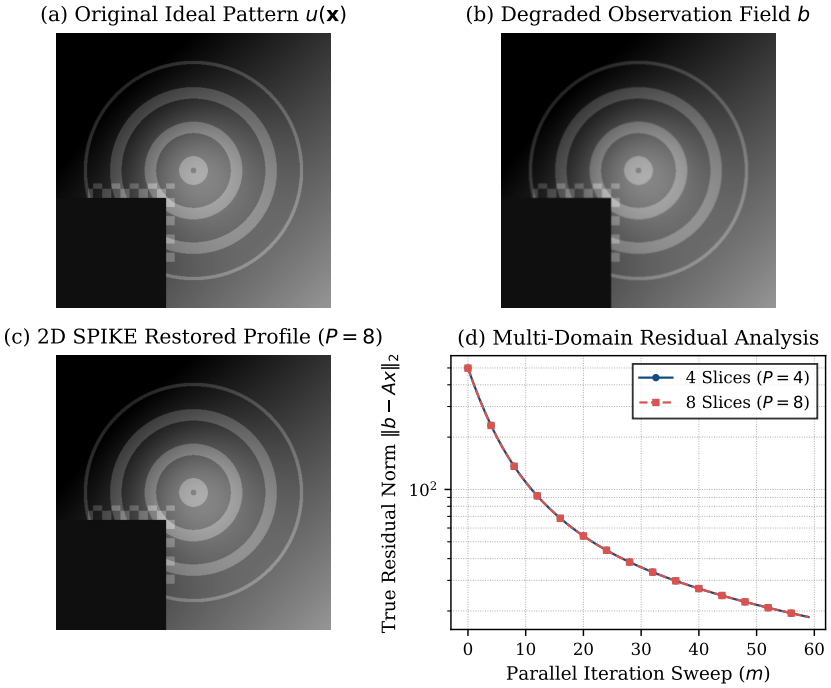


Figure 8: Image deblurring problem

6 Conclusion

In this work, we explored a novel unified parallel algorithm framework for solving obstacle problems on parallel computers. The variants of obstacle examples along with constrained quadratic programming models are investigated in the present study. A class of direct and indirect parallel algorithm are considered here. A rigorous mathematical justifications are established to prove the algorithm is numerically stable and achieve to its converged solution. Numerical exemplifications on multi-core computed nodes (distributed as well as shared) exhibit that the parallel algorithm compresses the spectral condition number of the discrete Laplacian operator. Robust asymptotic linear convergence is achieved down to machine tolerance within exceptionally low iteration cycles ensuring deadlock free network configurations. We have successfully retrieved robust computational result and independent redundant verification of a multi-dimensional solver framework driven by the distributed Line-Splitting SPIKE block-relaxation paradigm. We tested the algorithm across computational scenarios ranging from bounded 1D, 2D, and 3D elliptic obstacle partial differential equations

to a non-diagonally dominant 2D image deblurring optimization problems. The solver has demonstrated exceptional convergence stability, numerical reliability, and multidomain adaptability. In conclusion, the proposed stabilized unified parallel approach provides a mathematically rigorous, stable, and highly scalable algorithm for handling constrained multi-dimensional boundary-value operators. Future research directions will focus on extending the idea in the financial mathematics and optimal control problems.

Competing Interests

The authors declare that they have no competing interests.

Funding

The authors did not receive any specific funding support for the submitted work.

References

[1] Eric Polizzi and Ahmed H. Sameh, A parallel hybrid banded system solver: the SPIKE algorithm, *Parallel Computing 32 (2006) 177–194.*

[2] J.-L. Lions and G. Stampacchia. Variational inequalities. *Communications on Pure and Applied Mathematics*, 20(3):493–519, 1967.

[3] L. A. Caffarelli. The regularity of free boundaries in higher dimensions. *Acta Mathematica*, 139:155–184, 1977.

[4] F. Brezzi, W. Hager, and P.-A. Raviart. Error estimates for the finite element solution of variational inequalities. I. Primal methods. *Numerische Mathematik*, 28(4):431–443, 1977.

[5] R. Glowinski. *Numerical Methods for Nonlinear Variational Problems*. Springer-Verlag, New York, 1984.

[6] A. Veeser. Efficient and reliable a posteriori error estimators for elliptic obstacle problems. *SIAM Journal on Numerical Analysis*, 39(1):146–167, 2001.

[7] R. H. Nochetto, K. G. Siebert, and A. Veeser. Pointwise a posteriori error control for elliptic obstacle problems. *Numerische Mathematik*, 95(1):163–195, 2003.

[8] D. Braess, C. Carstensen, and R. H. W. Hoppe. Convergence of adaptive finite element methods for an obstacle problem. *Numerische Mathematik*, 107(3):455–471, 2007.

[9] T. Gudi. A remark on the a posteriori error analysis of discontinuous Galerkin methods for the obstacle problem. *Computational Methods in Applied Mathematics*, 14(1):71–81, 2014.

[10] R. S. Varga, *Matrix Iterative Analysis*, Springer Science & Business Media, 2nd ed., 2009.

[11] A. Weiss and B. Wohlmuth. A posteriori error estimator for a discontinuous Galerkin discretization of the obstacle problem. *SIAM Journal on Numerical Analysis*, 47(5):3613–3638, 2010.

[12] B. Ayuso de Dios, M. Brunetti, and I. Smears. Two new approaches for solving elliptic obstacle problems using discontinuous Galerkin methods. *BIT Numerical Mathematics*, 62:185–216, 2022.

[13] S. Gaddam and T. Gudi. A bubble-enriched quadratic finite element method for 3D elliptic obstacle problems. *Journal of Scientific Computing*, 73:251–275, 2017.

[14] M. P. Friedlander and P. Tseng. Exact regularization of convex programs. *SIAM Journal on Optimization*, 18(4):1326–1350, 2007.

[15] T. Goldstein and S. Osher. The split Bregman method for L^1-regularized problems. *SIAM Journal on Imaging Sciences*, 2(2):323–343, 2009.

[16] R. Glowinski. *Alternating Direction Methods of Multipliers: Insights and Applications*. SIAM, Philadelphia, 2016.

[17] M. Hintermüller, K. Ito, and K. Kunisch. The primal-dual active set strategy as a semismooth Newton method. *SIAM Journal on Optimization*, 13(3):865–888, 2003.

[18] L. Wang. Finite element error estimates for quadratic elements in obstacle problems. *Journal of Computational Mathematics*, 20(3):277–288, 2002.

[19] X. Wang, S. Ma, and H. Bi. A two-level finite element method for the elliptic obstacle problem. *Applied Mathematics and Computation*, 321:344–356, 2018.

[20] L. Badea, X.-C. Tai, and J. Wang. Convergence rate analysis of a multiplicative Schwarz method for variational inequalities. *SIAM Journal on Numerical Analysis*, 41(3):1052–1073, 2003.

[21] B. F. Smith, P. E. Bjørstad, and W. D. Gropp. *Domain Decomposition: Parallel Multilevel Methods for Elliptic Partial Differential Equations*. Cambridge University Press, 2004.

[22] A. Toselli and O. Widlund. *Domain Decomposition Methods—Algorithms and Theory*, volume 34. Springer Science & Business Media, 2005.

[23] C. Reisinger and J. Toivanen. A projected algebraic multigrid method for linear complementarity problems. *Numerical Mathematics: Theory, Methods and Applications*, 2(1):87–106, 2007.

[24] B. He. Parallel splitting augmented Lagrangian methods for monotone variational inequalities. *Computational Optimization and Applications*, 42(2):195–212, 2009.

[25] M. Tao and X. Yuan. An inexact parallel splitting augmented Lagrangian method for monotone variational inequalities with separable structures. *Computational Optimization and Applications*, 52(2):439–461, 2012.

[26] Spring, B. S., Polizzi, E., and Sameh, A. 2020. A feature-complete SPIKE dense banded solver. *ACM*

Trans. Math. Softw. 46, 4, Article 36 (Oct. 2020), 23 pages. https://doi.org

[27] Peeyush Singh, and Prawal Sinha *Interior-exterior penalty approach for solving Elastohydrodynamic Lubrication problem: Part I.*

[28] Tran, Giang and Schaeffer, Hayden and Feldman, William M and Osher, Stanley J, An L^1 penalty method for general obstacle problems, SIAM Journal on Applied Mathematics,vol. 75, No. 4,1424–1444, 2015.

[29] Peeyush Singh1 and Pravir Dutt, Total Variation Diminishing (TVD) method for Elastohydrodynamic Lubrication (EHL) problem on Parallel Computers, *The Journal of the Indian Mathematical Society, 91(1-2), 171–202.*

[30] Jianzhong Zhang , Naihua Xiu, New projection-type methods for monotone LCP with finite termination, *Numer. Math. (2002) 92: 179–195*

[31] Andreas Frommer and Rosemary A. Renaut. A unified approach to parallel space decomposition methods. *Journal of Computational and Applied Mathematics*, 110(1):205–223, 1999.

[32] M. C. Ferris and O. L. Mangasarian. Parallel variable distribution. *SIAM Journal on Optimization*, 4(4):815–832, November 1994.

[33] D. Kinderlehrer and G. Stampacchia. *An Introduction to Variational Inequalities and Their Applications*, volume 31 of *Classics in Applied Mathematics*. SIAM, 2000.

[34] J. L. Lions. The work of G. Stampacchia in variational inequalities. In F. Giannessi and A. Maugeri, editors, *Variational Analysis and Applications*, volume 79 of *Nonconvex Optimization and Its Applications*, pages 100–115. Springer, Boston, MA, 2005.

[35] R. Scholz. Numerical solution of the obstacle problem by the penalty method. *Computing*, 32(4):297–306, 1984.

[36] F. Brezzi, W. W. Hager, and P. A. Raviart. Error estimates for the finite element solution of variational inequalities. Part I: Primal theory. *Numerische Mathematik*, 28(4):431–443, 1977.

[37] Giang Tran, Hayden Schaeffer, William M. Feldman, and Stanley J. Osher. An L_1 penalty method for general obstacle problems. *SIAM Journal on Applied Mathematics*, 75(4):1424–1444, 2015.

[38] F. Wang, J. Eichholz, and W. Han. A two level algorithm for an obstacle problem. *Applied Mathematics and Computation*, 330:65–76, 2018.

[39] L. Wang. On the quadratic finite element approximation to the obstacle problem. *Numerische Mathematik*, 92(4):771–778, 2002.

[40] Thirupathi Gudi and Kamana Porwal. A posteriori error control of discontinuous Galerkin methods for elliptic obstacle problems. *Mathematics of Computation*, 83(286):579–602, 2014.